How to cite: *Angew. Chem. Int. Ed.* **2025**, e202515995
doi.org/10.1002/anie.202515995

Calcium Nanoparticles | Hot Paper

Redox Reactions with Calcium-Metal Nanoparticles

Christian Ritschel, Anja Appenzeller, Radian Popescu, Carsten Donsbach, Ralf Köppe, Jonas O. Wenzel, Frank Breher, Yolita M. Eggeler, Wim Klopper, and Claus Feldmann**

Abstract: Calcium is generally a highly reactive alkaline-earth metal, but as bulk metal, it exhibits only low reactivity at ambient conditions due to small surface area, low solubility, and/or passivation. The reactivity can be significantly enhanced when using small-sized calcium nanoparticles. In this regard, we describe the first synthesis of Ca(0) nanoparticles, 5.4 ± 1.2 nm in size, by TMEDA-supported reduction of CaI_2 with lithium naphthalenide in toluene (TMEDA: N,N,N′,N′-tetramethylethylenediamine). We also show Ca(0) nanoparticles to be substantially different from so-called "*Rieke calcium*". The high reactivity can be used for redox reactions, for instance, with $[Cp_2MoCl_2]$ and the sterically demanding β-diketiminate ligand H^{Dipp}NacNac (Dipp: 2,6-*i*$Pr_2C_6H_3$) or with $[(Ph_3P)AuCl]$ as a derivative of a ligand-stabilized noble metal. The Ca(0)-nanoparticle-driven reactions result in the novel compounds $[\{(^{Dipp}NacNac)(thf)Ca\}_2(naph)]$ (**1**) with a rare naphthalenide dianion, $[\{(^{Dipp}NacNac)(thf)CaMo(Cp)H\}_2(fulvalene)]$ (**2**) with unusual MoH → Ca dative bonding, and $[Au_9(PPh_3)_8](naph)(tmeda)_{0.5}$ (**3**) with a non-charged body-centered cubic Au_9 cluster core of zerovalent gold. Ca(0) nanoparticles and the compounds **1–3** are characterized by electron microscopy, X-ray diffraction (single crystals, powders), spectroscopy (IR, UV-Vis, NMR, EPR), and computation. Exemplarily, the formation of **1–3** points to the potential of nanosized alkaline-earth metals for chemical syntheses and the different reactivity of nanosized and bulk metals.

Introduction

In principle, the alkaline-earth metal calcium is highly reactive.[1] Qualitatively, the high reactivity is indicated by exothermal reactions with water, oxygen or halogen-containing organic solvents.[2] The high reactivity of calcium can be quantified based on its low electronegativity (1.0 on Pauling scale)[3] or its low electrochemical potential $[E^0_{bulk}(Ca/Ca^{2+}) = -2.84\ V]$.[4] In contrast to the expectation, bulk calcium shows only low reactivity at ambient conditions, which can be attributed to its low solubility, limited surface area, and surface passivation (e.g., by hydroxides, oxides, carbonates).[5] Activation of bulk calcium is possible, for instance, by dissolution in liquid ammonia, which, however, has the drawback of ammonia possibly reacting as base, ligand and/or oxidizing agent.[6] Recently, also ball-milling has proven to be efficient for activation and to obtain reactive Grignard reagents of the heavy alkali and alkaline-earth metals.[1,7,8]

The reactivity of calcium metal could be dramatically increased when using small-sized nanoparticles (< 10 nm) because of a significantly increased surface area and a great number of insufficiently coordinated surface atoms. Moreover, a passivation layer (usually 4–10 nm in thickness) cannot be formed for small-sized Ca(0) nanoparticles (≤ 5 nm).[9] Small-sized Ca(0) nanoparticles can also be considered to range at the border of heterogeneous and homogeneous conditions, which further promotes reactivity and reactions. In view of potential application, calcium particles were already discussed for high-voltage batteries, hydrogen storage or catalysis.[10–12] Furthermore, alkaline-earth compounds with low-valent oxidation states such as Mg(0) and Ca(I) were recently reported in basic science as unique pieces of the chemical cabinet.[13–15] The knowledge on Ca(0) nanoparticles, however, is very limited until now. Most often, Ca(0) particles with large size (> 100 nm), broad size distribution, and/or significant agglomeration were obtained via physical methods[16,17] or metal vaporization followed by deposition into inert liquid media (e.g., THF/hexadecylamine).[18] Moreover, deposition of calcium from liquid ammonia on glass spheres was described.[15,19] Finally, so-called *"Rieke calcium"* is known and obtainable by reaction of CaI_2 and lithium naphthalenide or lithium biphenylide in THF.[20–24] Although the specific composition of *"Rieke calcium"* is unclear, the deep black compounds are considered to consist of Ca(II) and naphthalenide or biphenylide radical anions.[24,25] Ca(0)

[*] Dr. C. Ritschel, Dr. C. Donsbach, Dr. R. Köppe, Dr. J. O. Wenzel, Prof. Dr. F. Breher, Prof. Dr. C. Feldmann
Institute of Inorganic Chemie, Karlsruhe Institute of Technology (KIT), Engesserstraße 15, D-76131 Karlsruhe, Germany
E-mail: claus.feldmann@kit.edu

A. Appenzeller, Prof. Dr. W. Klopper
Institute of Physical Chemistry, Karlsruhe Institute of Technology (KIT), Fritz-Haber-Weg 2, 76131 Karlsruhe, Germany
E-mail: klopper@kit.edu

Dr. R. Popescu, Prof. Dr. Y. M. Eggeler
Laboratory for Electron Microscopy, Karlsruhe Institute of Technology (KIT), Engesserstrasse 7, D-76131 Karlsruhe, Germany

Additional supporting information can be found online in the Supporting Information section

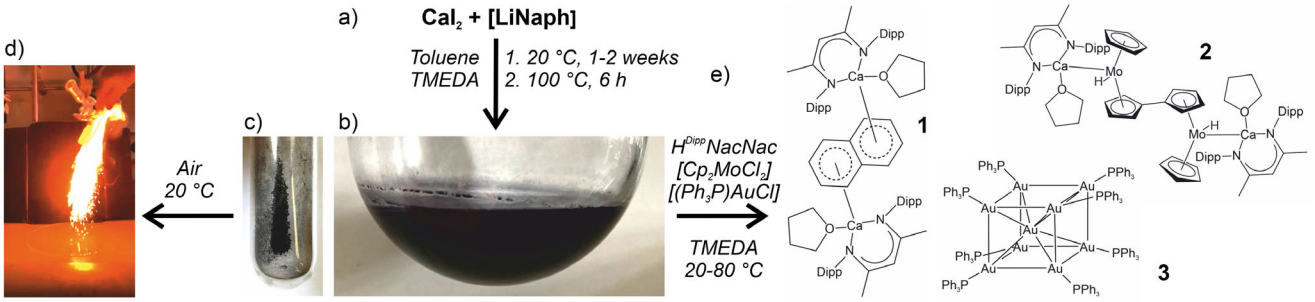

Figure 1. Ca(0) nanoparticles and their reactions: a) scheme of synthesis with b) photo of suspension and c) powder of Ca(0) nanoparticles, d) reaction of Ca(0) nanoparticle powder in air, e) compounds **1–3** after reaction of Ca(0) nanoparticles with H^{Dipp}NacNac, $[Cp_2MoCl_2]$/H^{Dipp}NacNac, and $[(Ph_3P)AuCl]$.

nanoparticles with uniform, small size (< 50 nm) as well as a liquid-phase synthesis, to the best of our knowledge, have not been described until now.

In the following, we first present a liquid-phase synthesis of crystalline Ca(0) nanoparticles with a diameter of 5.4 ± 1.2 nm. The high reactivity of the Ca(0) nanoparticles can be utilized in the liquid phase to perform redox reactions at the border of homogeneous and heterogeneous conditions, for instance, with $[Cp_2MoCl_2]$ in the presence of the sterically demanding β-diketiminate ligand H^{Dipp}NacNac or with $[(Ph_3P)AuCl]$ as a derivative of a ligand-stabilized noble metal and results in three novel compounds.

Results and Discussion

Synthesis of Ca(0) Nanoparticles

Base-metal nanoparticles have generally attracted our interest.[26–28] In particular, the reduction of metal halides by alkali-metal naphthalenides ([LiNaph], [NaNaph]) in THF has been proven to be a versatile synthesis strategy to obtain the group 3-to-group 6 transition metals and all lanthanide metals (La to Lu) with a size of 1–5 nm.[29,30] Whereas this strategy was also successful for Mg(0) nanoparticles (i.e., reduction of $MgBr_2$ with [LiNaph] in THF),[31] it failed for calcium. Thus, a reduction of CaI_2 with [LiNaph] in THF only led to deep black calcium naphthalenide (*SI*: Section 3), which compares to *"Rieke calcium"*.[20–25] Infrared spectroscopy (FT-IR), elemental analysis (C/H/N analysis), and total organics combustion indicate a composition $[Ca^{2+}(naph)^{2-}(thf)_2]$ (*SI*: Table S1, Figures S1–S7) with a coordination of Ca^{2+} by THF and $(naph)^{2-}$ being obviously preferred over the reduction to zerovalent calcium.

Aiming at Ca(0) nanoparticles, we have selected toluene as solvent, wherein, however, CaI_2 and [LiNaph] are both insoluble. Therefore, [LiNaph] was first coordinated by N,N,N′,N′-tetramethylethylenediamine (TMEDA) to become soluble in toluene (Figure 1a). Thereafter, CaI_2 can be added either with or without prior coordination by TMEDA. Here, the addition of pure CaI_2 is preferred to limit the total TMEDA concentration. The nucleation of Ca(0) nanoparticles was successful with these specific conditions since the dissolution of CaI_2 is very slow, while its reduction after dissolution by [LiNaph] is very fast. Calcium metal is insoluble in toluene, which causes a high supersaturation and, thus, promotes the formation of small-sized particles.[32] Successful reduction and nucleation of Ca(0) nanoparticles is indicated by the formation of a deep-black suspension with slightly bluish appearance (Figure 1b). These as-prepared Ca(0) nanoparticles are very small (1–3 nm) and extremely reactive but difficult to separate via centrifugation (*SI*: Figures S8–S11). Therefore, we also applied certain heating (100 °C) to slightly increase the size of the Ca(0) nanoparticles (5.4 ± 1.2 nm). This also decreases the amount of organics (toluene, naphthalene, THF, TMEDA) adsorbed on the particle surface (*SI*: Figures S12–S16).

Finally, the Ca(0) nanoparticles were purified by centrifugation and repeated redispersion/centrifugation in/from THF and toluene to remove remaining starting materials, naphthalene, TMEDA and LiI (*SI*: Figures S14–S18). Thereafter, they were either dried in vacuum at room temperature to obtain powder samples (Figure 1c), or they were redispersed in toluene or TMEDA to obtain suspensions for further reactions. It should be noticed that handling of the Ca(0) nanoparticles requires specific attention as they show instantaneous combustion in air and even explosion when in contact to water or other oxidizing agents (Figure 1d).

Characterization of Ca(0) Nanoparticles

The as-prepared Ca(0) nanoparticles exhibit a uniform spherical shape with a size in the 5 nm-range and a low degree of agglomeration (Figure 2a). Statistical evaluation of > 60 Ca(0) nanoparticles on TEM images resulted in a mean particle diameter of 5.4 ± 1.2 nm (Figure 2b; for more images, see *SI*: Figure S12). High-resolution (HR)TEM images confirm the presence and crystallinity of the Ca(0) nanoparticles, which show lattice fringes extending through the whole particle (Figure 2c). The observed average lattice-fringe distance of 2.8 ± 0.1 Å is in agreement with face-centred cubic (*fcc*) bulk calcium (d_{020} = 2.8 Å) (*SI*: Figures S12, S13).[33] The two-dimensional Fourier transform (FT) pattern of the nanoparticle on the HRTEM image (Figure 2c) is also

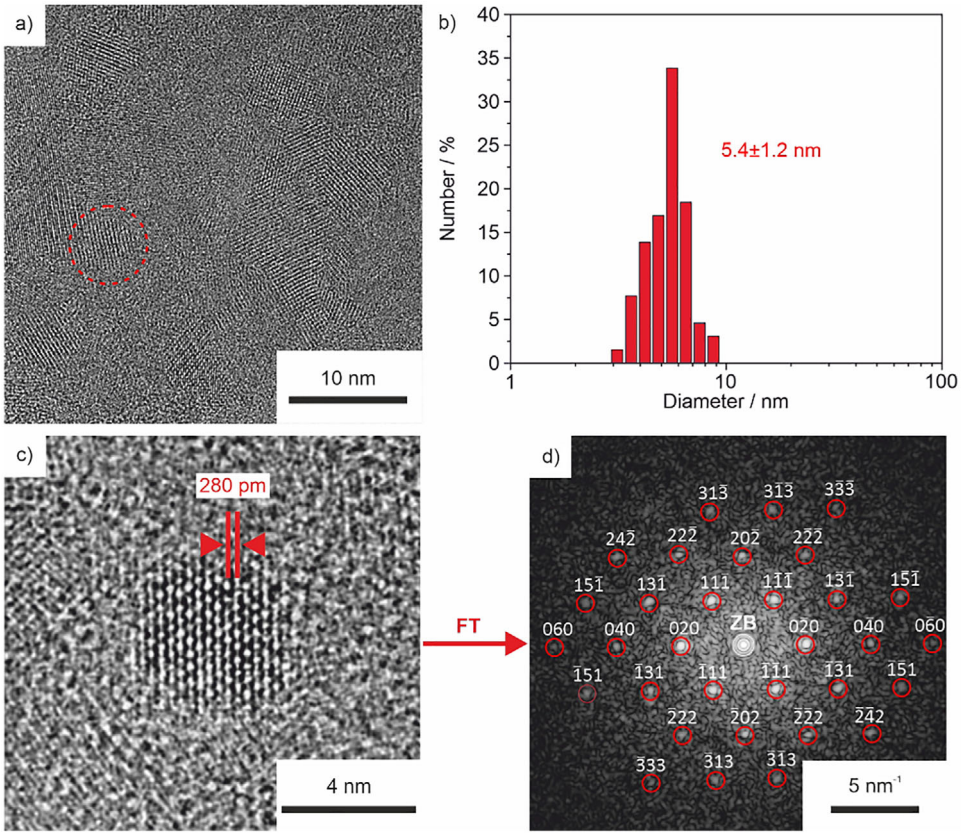

Figure 2. Electron microscopy of the as-prepared Ca(0) nanoparticles: a) HRTEM overview image with single nanoparticle indicated by red dots (*for more images see SI*: Figure S12), b) size distribution (according to a statistical evaluation of > 60 nanoparticles on HRTEM images), c) HRTEM image of a single nanoparticle with lattice fringes, d) FT pattern of single nanoparticle shown in (c) agrees with the calculated diffraction pattern of the *fcc*-bulk Ca (red circles and Miller indices) in the [101] zone axis (zero-order beam, ZB, marked by white circle).

in agreement with the calculated diffraction pattern of *fcc*-bulk calcium within the [101]-zone axis (Figure 2d).[33] It should also be noticed that HRTEM images did not show any calcium-oxide species. The crystallinity of the Ca(0) nanoparticles is further confirmed by calculating the FT of a Ca(0) nanoparticle ensemble with different orientations on HRTEM images recorded at low magnification (*SI*: Figure S13).

The crystallinity of the Ca(0) nanoparticles was also examined by X-ray powder diffraction (XRD). However, no Bragg reflexes are observed, which can be ascribed to the small particle size (5.4 ± 1.2 nm) and the resulting low scattering power (*SI*: Figure S14).[29,30] Moreover, it should be noticed that no impurities occur (e.g., LiI, CaI_2, CaO, $Ca(OH)_2$). Fourier-transform infrared (FT-IR) spectroscopy, elemental analysis (C/H/N analysis), and total organics combustion were applied to elucidate the surface functionalization of the Ca(0) nanoparticles. FT-IR spectra show only weak vibrations of toluene and naphthalene (1575, 1238, 734 cm^{-1}); vibrations of TMEDA are absent (*SI*: Figures S15–S18). Most importantly, the vibrations observed for the Ca(0) nanoparticles are significantly different from calcium naphthalenide/"*Rieke calcium*" (*SI*: Figures S5, S6). C/H/N analysis and total organics combustion confirm the surface functionalization with toluene and naphthalene in the range of a monolayer (*SI*: Sections 4,5) and, again, prove the Ca(0) nanoparticles to be substantially different from calcium naphthalenide/"*Rieke calcium*" (*SI*: Sections 4,5).

Reactivity and Reactions of Ca(0) Nanoparticles

The reactivity of the Ca(0) nanoparticles is already indicated when in contact to air or water, which leads to immediate combustion and/or explosion (Figure 1d; *SI*: Figure S19). Strong reactions are specifically observed for powder samples, whereas the Ca(0) nanoparticles are chemically and colloidally stable under inert conditions as suspension in toluene or TMEDA. The fact that long-chained or high-molecular-weight stabilizers (such as oleylamine, oleic acid, polyethylene glycol) are absent is a specific advantage of the Ca(0) nanoparticles for syntheses. To probe their reactivity, the Ca(0) nanoparticles were here exemplarily reacted with $[Cp_2MoCl_2]$ and the sterically demanding β-diketiminate ligand H^{Dipp}NacNac as well as with $[(Ph_3P)AuCl]$ as a derivative of a ligand-stabilized noble metal.

[{(^{Dipp}NacNac)(thf)Ca}$_2$(naph)] (1). ^{Dipp}NacNac (i.e., $HC[C(Me)N(2,6\text{-}^{i}Pr\text{-}C_6H_3)]_2$, N-{(2Z,4E)-4-[(2,6-diisopropylphenyl)imino]-2-penten-2-yl}-2,6-diisopropylaniline)

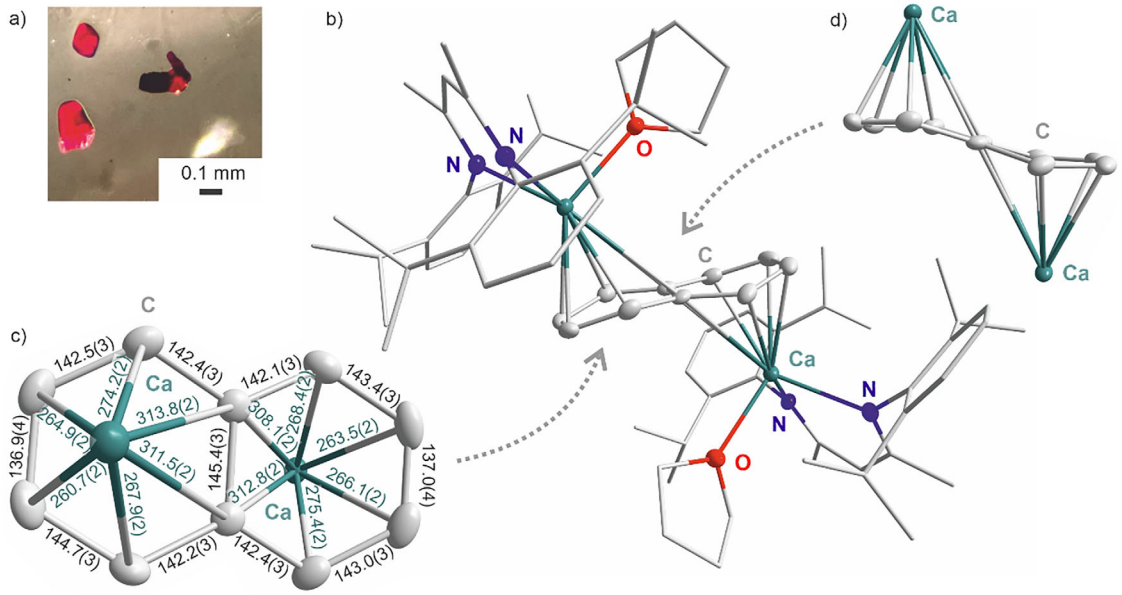

Figure 3. [{(^{Dipp}NacNac)(thf)Ca}$_2$(naph)] (**1**) with: a) photo of single crystals, b) molecular structure, c + d) tilted $(naph)^{2-}$ ligand with top-view and C—C distances in pm (c) as well as side-view (d).

is well-known as a sterically demanding, chelating β-diketiminate ligand that allows to prepare unique compounds with extraordinary bonding situations.[34] Prominent examples include [{(^{Dipp}NacNac)Mg(I)}$_2$], [^{Dipp}NacNacAl(I)], or {[(BDI*)Mg$^-$][Na$^+$]}$_2$ (BDI*: HC{C(*t*Bu)N[2,6-(3-pentyl)-phenyl]}$_2$).[14,35,36] These specific features motivated us to probe the reactivity of the Ca(0) nanoparticles with ^{Dipp}NacNac with comparable conditions. By reaction of Ca(0) nanoparticles, H^{Dipp}NacNac and few drops of TMEDA in a glass ampoule for one week at 25 °C, red block-shaped crystals were obtained (Figure 3a). Single-crystal structure analysis revealed a composition [{(^{Dipp}NacNac)(thf)Ca}$_2$(naph)] (**1**) with a $(naph)^{2-}$ ligand sandwiched by two {(^{Dipp}NacNac)(thf)Ca}$^+$ units (Figures 1e,3b; *SI*: Figure S20). The tendency of calcium to form anionic naphthalenide compounds was already observed with [$Ca^{2+}(naph)^{2-}(thf)_2$] nanoparticles from the THF-based synthesis (*SI*: Section 3). Here, it should be noticed that **1** was only obtained when using the as-prepared, non-heated Ca(0) nanoparticles, which might be due to their even smaller particle size and the, therefore, higher amount of naphthalene adsorbed on the particle surface (*SI*: Section 4).

1 crystallizes in the monoclinic space group $P2_1$ (*SI*: Table S2, Figure S21). Even though the structure of **1** looks centrosymmetric at first sight, the position of several light atoms leads to symmetry reduction. The Ca–C distances to the $(naph)^{2-}$ ligand show significant variation, which can be ascribed to its tilted structure with angles of 15.7(1)° and 16.9(2)° between the planes (Figure 3c; *SI*: Figure S20). For each of the two 6-membered rings, four shorter Ca–C distances [260.7(2)-275.4(2) pm] and two longer Ca–C distances [308.1(2)-313.8(2) pm] are observed (Figure 3d; *SI*: Table S3), resulting in a η^{4+2} coordination to calcium. FT-IR spectra confirm the presence of dianionic naphthalenide, ^{Dipp}NacNac, and THF in **1** (*SI*: Figure S22). UV-Vis spectra are in agreement with the red color of **1** (Figure 3a; *SI*: Figure S23). With (^{DIPeP}BDI)Ca(μ^4,μ^4-naphthalene)Ca(^{DIPeP}BDI) and the heterobimetallic inverse Mg/Ca sandwich compounds [(^{DIPeP}BDI*)Mg(μ^2,μ^4-naphthalene)Ca(^{DIPeP}BDI)] (^{DIPeP}BDI: HC[C(Me)N-DIPeP]$_2$; ^{DIPeP}BDI*: HC[C(*t*Bu)N-DIPeP]$_2$; DIPeP: 2,6-CH(Et)$_2$-phenyl), recently, two comparable compound were realized by Harder et al. by reduction of [(^{DIPeP}BDI)CaI]$_2$ with KC_8.[37,38] With ^{DIPeP}BDI, however, a sterically even more demanding NacNac ligand was used. Beside these compounds, **1** is the only compound with calcium coordinated by a $(naph)^{2-}$ ligand until now. A $(naph)^{2-}$ dianion is rare, in general, and yet only known for few metals (i.e., alkali metals, rare-earth metals).[39–43]

[{(^{Dipp}NacNac)(thf)CaMo(Cp)H}$_2$(fulvalene)] (2). As a next example, we reacted the Ca(0) nanoparticles and H^{Dipp}NacNac with few drops of TMEDA in the presence of [Cp_2MoCl_2]. After 2 weeks at 80 °C, red-orange crystals (Figure 4a; *SI*: Table S2) of [{(^{Dipp}NacNac)(thf)CaMo(Cp)H}$_2$(fulvalene)] (**2**) were obtained that consist of a {Mo_2(fulvalene)Cp_2H_2} unit, sandwiched by two {Ca(^{Dipp}NacNac)(thf)} units (Figures 1e,4b; *SI*: Tables S4, S5, Figures S24–S31).

Fulvalen is an intensely studied ligand in transition-metal chemistry[44] and, in particular, the chemistry of molybdenum.[45] Thus, [Mo_2(fulvalen)Cp_2H_2][46] and [Mo_2(fulvalen)Cp_2H_4][47] exhibit comparable building units as **2** (*SI*: Figure S27). [Mo_2(fulvalen)Cp_2H_2] shows Mo–Mo bonding,[46] whereas [Mo_2(fulvalen)Cp_2H_4] exhibits an unusual *anti*-conformation without Mo–Mo bonding.[47] Such *anti*-conformation is also observed for **2**. This raises the question if the Mo atoms in **2** are also coordinated by hydride ligands as in [Mo_2(fulvalen)Cp_2H_2] or [Mo_2(fulvalen)Cp_2H_4] (*SI*: Table S5), which can be hardly answered by single-crystal structure analysis. Residual electron density at the Mo site,

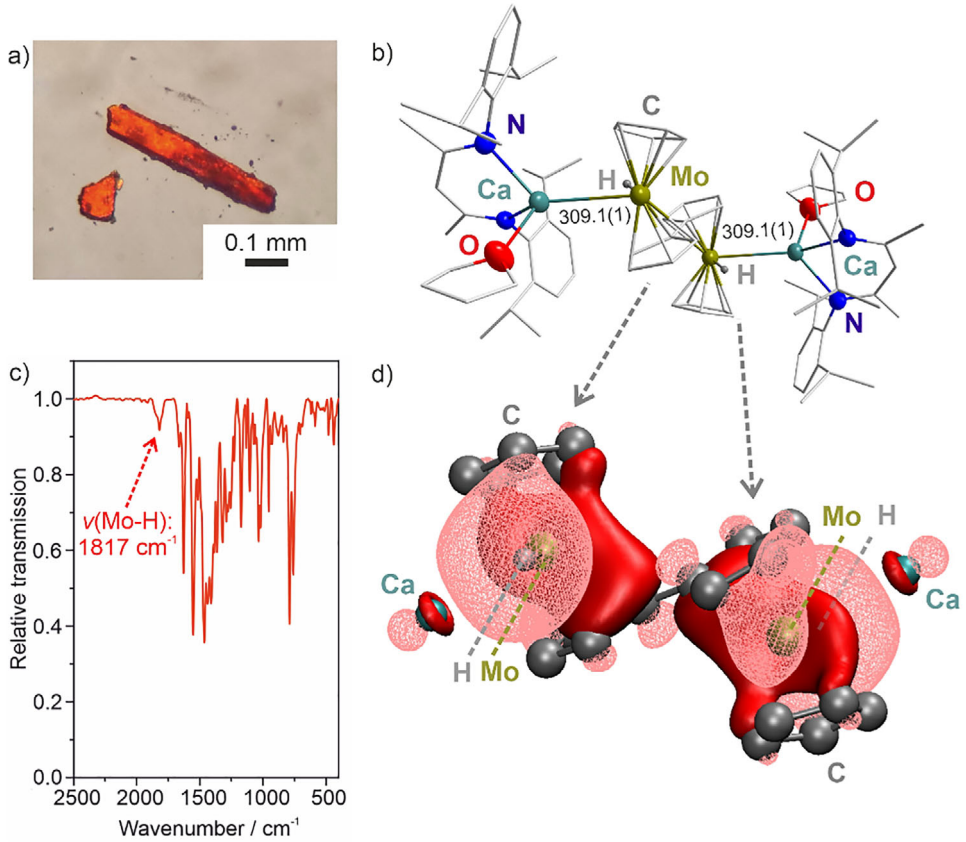

Figure 4. [{(^{Dipp}NacNac)(thf)CaMo(Cp)H}$_2$(fulvalene)] (**2**) with: a) photo of single crystals, b) molecular structure with MoH → Ca dative bonding (distances in pm), c) cutout of FT-IR spectrum with ν(Mo–H) vibration (see *SI*: Figure S28 for complete FT-IR spectrum); d) two localized orbitals obtained with the PBE0 functional and shown as red and transparent red isosurfaces at values of ± 0.02 $a_0^{-3/2}$.

however, already points to the presence of hydride ligands. Synthetically, hydride ligands can originate from a reduction of H^{Dipp}NacNac or Cp as well as, most probably, from the formation of fulvalene. In the literature, Mo–Cp distances of $MoCp_2$ units without and with hydride ligands were reported to be > 197 pm and < 195 pm,[48–50] respectively, which suggests the presence of hydride ligands in **2** (Mo–Cp: 191.1(1) pm). FT-IR spectra of **2** clearly indicate a ν(Mo–H) vibration (1817 cm^{-1}) similar to [Mo_2(fulvalen)Cp_2H_2] (1829 cm^{-1}) (Figure 4c; *SI*: Figure S28).[46,47] Moreover, the ^{1}H NMR spectrum of **2** in C_7D_8 shows a characteristic hydride signal at $\delta = -9.3$ ppm (*SI*: Figures S29, S30).[46,47] The absence of any coupling to other hydrogen atoms confirms each Mo atom to be coordinated by a single hydride ligand. Density functional theory (DFT) calculations further support the presence of one hydride ligand per Mo atom (Figure 4d; SI: Figures S38–S43).

An even more interesting feature of **2** relates to the remarkably short Mo─Ca distance of 309.1(1) pm (Figure 4b; *SI*: Table S4), which – to the best of our knowledge – is the shortest Mo─Ca distance observed until now. The short distance is also reflected by computation (301.0 pm based on PBE-D3(BJ) level; *SI*: Table S8). The Mo─Ca distance in **2** is shorter than the summed covalent radii of Mo and Ca (reported with 309 and 330 pm)[51,52] and, thus, in the range of a covalent bond. Comparable findings were reported for short Mo─Mg distances (summed covalent radii Mg/Mo reported with 277 and 295 pm),[51,52] including [Cp_2Mo(H)MgBr(thf)$_2$] (Mo─Mg: 273.2 pm)[48] or [(Cp_2MoH)Mg(Et_2O)(iPrMg)Br_2]$_2$ (Mo─Mg: 273.7 pm)[53] (*SI*: Figure S27). In the case of Mg, an ionic interaction is suggested as a contribution of *d* orbitals is less probable.[54–57] In recent studies, *d*─*d* dative bonding between transition metals and the heavier alkaline-earth metals Ca, Sr, and Ba with electron density of *d* orbitals of the transition metal transferred to empty *d* orbitals of the heavier alkaline-earth metal was discussed.[58–60] In this regard, quantum-chemical calculations suggested Fe→Ca *d*–*d* dative bonding in the [CaFe(CO)$_{10}$]$^+$ cation[33a,b] (*d*(Ca─Fe): 309.6 pm; sum of covalent radii: 287 and 308 pm)[51,52] or in a substituted ferrocene complex (*d*(Ca–Fe): 311.3 pm; sum of covalent radii: 287 and 308 pm)[51,52] (*SI*: Figure S27).[60] For **2**, the orbitals were localized by means of the Pipek-Mezey approach,[61] and the two most interesting localized molecular orbitals (LMOs) are shown in Figure 4d (*SI*: Figure S39). These two LMOs may be considered as two-electron-two-center bonds built mainly from the 1*s* atomic orbital of H and a 4*d* atomic orbital of Mo, with a small contribution of the 4*s* atomic orbital of Ca, as can be concluded from the Mulliken populations of the LMO, which are 0.89 for Mo, 0.97 for H, and 0.14 for Ca. In view of the Ca population, therefore, we interpret the LMO as a MoH─Ca dative bond, as a charge of

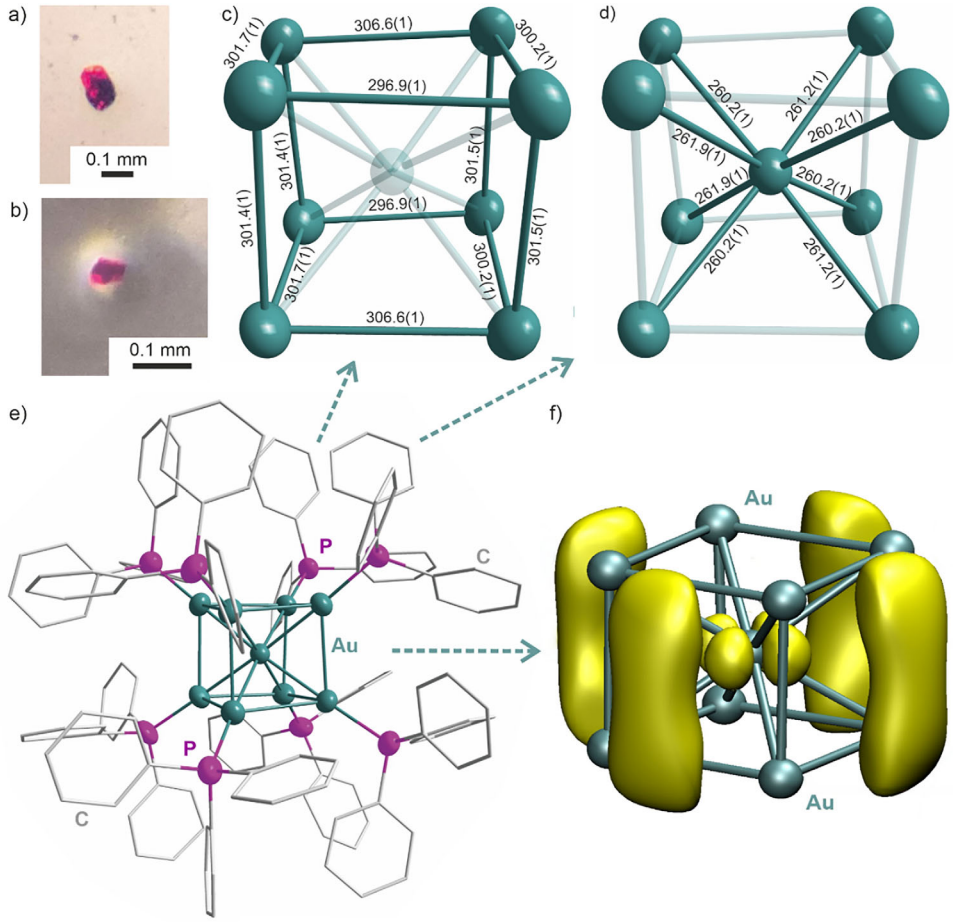

Figure 5. $[Au_9(PPh_3)_8](naph)(tmeda)_{0.5}$ (**3**) with: a + b) photos of single crystals, c + d) Au_9 cluster core with Au_{corner}–Au_{corner} distances in pm (c) and with Au_{center}–Au_{corner} distances in pm (d); e) molecular structure; f) spin density computed at the TPSSh/def2-SV(P) level and plotted with an isovalue of 0.001 a_0^{-3}.

–0.14 *e* was transferred from the MoH σ-bond to the Ca^{2+} ion, which is comparable to the interaction observed for ZnH–TM bonding (TM: transition metal).[62]

$[Au_9(PPh_3)_8](naph)(tmeda)_{0.5}$ (3). As a third example, we have reacted the Ca(0) nanoparticles with $[(Ph_3P)AuCl]$ as a derivative of a ligand-stabilized noble metal. This was performed with Ca(0) nanoparticles and $[(Ph_3P)AuCl]$ in few drops of TMEDA, which, after 3 weeks at 80 °C, resulted in tiny deep-red, block-shaped crystals (Figure 5a,b). According to single-crystal structure analysis, **3** crystallizes in the monoclinic space group *C2/c* and consists of $[Au_9(PPh_3)_8]$ cluster units with naphthalene and TMEDA in between (*SI*: Table S2, Figures S32–S35). The $[Au_9(PPh_3)_8]$ unit contains a body-centred cubic (*bcc*) arrangement of gold atoms with Au_{center}–Au_{corner} of 260.2(1)-262.0(1) pm and Au_{corner}–Au_{corner} distances of 296.9(1)-306.6(1) pm (Figures 1e,5c-e; *SI*: Table S6). The Au_{corner}–Au_{corner}–Au_{corner} angles (86.4(1)-93.6(1)°) indicate slight deviation from an ideal cube (*SI*: Table S7).

The reduction of $[(PPh_3)AuCl]$ (e.g., with $(PPh_3)BH_3$, $NaBH_4$, GaCp)[63–65] to obtain gold clusters such as $[Au_9(PPh_3)_8]Cl$, $[Au_{11}(PPh_3)_7]Cl_3$, and $[(PPh_3)_8Au_9GaCl_2][GaCl_4][GaCpCl_3]$ is well-known, in principle, and motivated us to probe comparable conditions with Ca(0) nanoparticles. This approach – using metal nanoparticles as a starting material – is here applied for the first time. At first sight, $[Au_9(PPh_3)_8]Cl$ (Au_{center}–Au_{corner}: 260.6(1)-261.8(1) pm; Au_{corner}–Au_{corner}: 300.0(1)-304.2(1) pm; Au_{corner}–Au_{corner}–Au_{corner} 88.8(1)-90.4(1) °)[63] is similar to **3** (*SI*: Tables S6, S7). $[Au_9(PPh_3)_8]Cl$ was described as ionic compound with $[Au_9(PPh_3)_8]^+$ cations and Cl^- anions but with weak evidence for the presence of chlorine (*SI*: Section 6).[63] Interestingly, the $[Au_9(PPh_3)_8]^+$ cation was reported for low stability with fast conversion to $[Au_{11}(PPh_3)_8Cl_2]^+$.[63]

Based on the aforementioned literature data, **3** could be denoted as saline $[Au_9(PPh_3)_8]^+(naph)^-(tmeda)_{0.5}$ or non-charged $[Au_9(PPh_3)_8](naph)(tmeda)_{0.5}$. To differentiate both, the red color of **3** is already indicative (Figure 5a,b; *SI*: Figure S36). Such color is often observed for gold clusters[63–65] and in accordance with colorless naphthalene, whereas a $(naph)^-$ radical anion would add a deep green color, which – due to additive color mixing – would result in a dark/black color of **3**. This view is supported by continuous-wave electron paramagnetic resonance (cw-EPR) spectroscopy at X-band (~9 GHz), which does not show any signal around the *g* value of 2 as indicative for an organic

radicals like the $(naph)^-$ radical anion (*SI*: Figure S37).[66,67] The Au_9 cluster core itself should also exhibit an unpaired electron but the corresponding EPR signals are well-known to be broad and often undetectable in conventional isotropic X-band EPR spectroscopic measurements.[68,69] Moreover, the characteristic and intense out-of-plane bending vibration is suitable to differentiate non-charged naphthalene and a $(naph)^-$ radical anion (*SI*: Section 6). For **3**, this vibration is observed at 787 cm^{-1} (*SI*: Figure S34) and in good agreement with non-charged naphthalene (experimental: 783 cm^{-1}, *SI*: Figure S34; theory: 789 cm^{-1}, *SI*: Figure S35; literature: 789 cm^{-1}),[70,71] whereas the out-of-plane bending vibration of the $(naph)^-$ radical anion is at 692 cm^{-1} (*SI*: Figure S34) (theory: 662 cm^{-1}, *SI*: Figure S35; literature: 715 cm^{-1}).[70,71] Finally, DFT calculations consistently show that **3** has one unpaired electron (Figure 5e; *SI*: Table S9, Figure S44). Clearly, the spin density is located on the $[Au_9(PPh_3)_8]$ cluster, and within the cluster mainly on the Au centers. A natural population analysis[72] yielded a population of about 0.05 majority-spin electrons in a 5*d* orbital of the central Au atom and populations of about 0.08 majority-spin electrons in 5*p* orbitals of the other eight Au atoms. According to DFT calculations, **3** is also more stable with non-charged naphthalene in terms of reaction energy (−76 kJ mol^{-1}) and electron affinity (−161 kJ mol^{-1}) than with a $(naph)^-$ radical anion (*SI*: Section 7).

With the results of crystal-structure analysis, UV-Vis/EPR/FT-IR spectroscopy, and DFT calculations (*SI*: Section 6), **3** can be consistently summarized to contain a non-charged $[Au_9(PPh_3)_8]$ molecule with a *bcc* Au_9 cluster core. Thus, **3** adds to the still small group of compounds containing zerovalent gold, including the dimer $PPh_3Au_2PPh_3$ as well as the cluster compounds $[Au_{20}(^tBu_3P)_8]$ and $[Au_{22}(Ph_2P(CH_2)_8PPh_2)_6]$.[73–75]

Conclusion

Calcium, Ca(0), nanoparticles are obtained by reduction of CaI_2 with [LiNaph] in toluene. In contrast to other reactive base-metal nanoparticles (i.e., group 3-to-group 6 transition metals, lanthanide metals), a reduction of Ca^{2+} in THF is not possible, which can be ascribed to the even more negative electrochemical potential of calcium [$E^0_{bulk}(Ca/Ca^{2+}) = -2.84$ V]. As CaI_2 and [LiNaph] are insoluble in toluene, coordination of at least one of them by N,N,N′,N′-tetramethylethylenediamine (TMEDA) is necessary. Thus, the realization of Ca(0) nanoparticles requires an advanced strategy in comparison to our already reported synthesis of base-metal nanoparticles. As a result, monocrystalline Ca(0) nanoparticles with a size of 5.4 ± 1.2 nm are obtained in the liquid phase. We can also clearly differentiate the as-prepared Ca(0) nanoparticles from so-called *"Rieke calcium"* made from [LiNaph], which – as indicated by spectroscopy and chemical composition – represents the calcium naphthalenide $[Ca(naph)(thf)_2]$ without any zerovalent calcium.

The reactivity of the Ca(0) nanoparticles is significantly higher than for bulk calcium and allows to perform redox reactions at moderate temperature (20°C–80 °C). Exemplarily, the Ca(0) nanoparticles are reacted with $[Cp_2MoCl_2]$ and the sterically demanding β-diketiminate ligand $H^{Dipp}NacNac$ as well as with $[(Ph_3P)AuCl]$ as a derivative of a ligand-stabilized noble metal. These reactions result in the formation of $[\{(^{Dipp}NacNac)(thf)Ca\}_2(naph)]$ (**1**), $[\{(^{Dipp}NacNac)(thf)CaMo(Cp)H\}_2(fulvalene)]$ (**2**) and $[Au_9(PPh_3)_8](naph)(tmeda)_{0.5}$ (**3**). **1** is a rare example of a compound containing a tilted dianionic $(naph)^{2-}$ ligand. **2** exhibits an unusual MoH → Ca dative bond with electrons of the Mo–H bond shifted to the empty 4*s* orbital of Ca. Finally, **3** contains a non-charged body-centred cubic Au_9 cluster core with zerovalent gold. Besides the liquid-phase synthesis and characterization of small-sized Ca(0) nanoparticles (< 10 nm), generally, the potential of Ca(0) nanoparticles is shown to perform redox reactions at moderate temperature in the liquid phase.

Author Contributions

C.R. performed the synthesis and the material characterization, collected the data and wrote the manuscript draft. C.D. performed the refinement of the single-crystal structures. J.O.W. and F. Breher performed EPR investigations. R.P. and Y.M.E. performed advanced TEM analysis and contributed to the paper draft. A.A. and W.K. performed and evaluated DFT calculations and contributed to the paper draft. C.F. supervised the project, wrote and finalized the manuscript.

Acknowledgements

C.R. and C.F. thank Dr. F. Jung and J. Treptow for performing TEM analysis at the FEI Osiris ChemiSTEM. The authors also thank Dr. S. Wolf for refinement of structural details and H. Gröger for excellent laboratory assistance. Furthermore, C.R., W.K., and C.F. acknowledge the Deutsche Forschungsgemeinschaft (DFG) for funding within the collaborative research center "4f for Future (projects A4 and Q)". The authors thank Dr. M. T. Gamer and Prof. Dr. P. W. Roesky for data collection of compound **1** on a Stoe StadiVari diffractometer with Mo-microfocus source. Moreover, the authors acknowledge the Karlsruhe Nano Micro Facility (KNMF) and Prof. Dr. D. Fenske for data collection of compound **3** on a Stoe StadiVari diffractometer with Ga-metal-jet source. Finally, C.R. acknowledges the Studienstiftung des Deutschen Volkes for PhD scholarship.

Conflict of Interests

The authors declare no conflict of interest.

Data Availability Statement

Details regarding analytical techniques, starting materials and syntheses, characterization of calcium naphthalenide $[Ca(naph)(thf)_2]$, characterization of the Ca(0) nanoparticles, as well as the crystallographic data and more details for

the characterization of the compounds **1**–**3** can be found in the Supporting Information. Further details related to the crystal structures of **1**–**3** may be also obtained from the joint CCDC/FIZ Karlsruhe deposition service on quoting the depository numbers 2467344 (**1**), 2467343 (**2**), and 2467345 (**3**).

Keywords: Calcium nanoparticles · Crystal-structure analysis · Dative bonding · Gold cluster · Reactivity

[1] P. Gao, J. Jiang, S. Maeda, K. Kubota, H. Ito, *Angew. Chem. Int. Ed.* **2022**, *61*, e202207118, https://doi.org/10.1002/anie.202207118.

[2] R. C. Ropp, *Encyclopedia of the Alkaline Earth Compounds*, Elsevier, Oxford **2013**.

[3] N. Wiberg, E. Wiberg, A. F. Holleman, *Anorganische Chemie*, de Gruyter, Berlin **2017**, 103. Ed., Vol. *1*, Annex III/IV.

[4] N. Wiberg, E. Wiberg, A. F. Holleman, A. Chemie, de G., Berlin **2007**, 102. Ed., Table III.

[5] P. Marcus, V. Maurice, *Mater. Sci. Technol.* **2000**, *19*, 131–169.

[6] G. Moesges, F. Hampel, M. Kaupp, P. v. R. Schleyer, *J. Am. Chem. Soc.* **1992**, *114*, 10880–10889, https://doi.org/10.1021/ja00053a026.

[7] S. Harder, J. Langer, *Nature Rev. Chem.* **2023**, *7*, 843–853, https://doi.org/10.1038/s41570-023-00548-0.

[8] D. Jędrzkiewicz, J. Mai, J. Langer, Z. Mathe, N. Patel, S. DeBeer, S. Harder, *Angew. Chem. Int. Ed.* **2022**, *61*, e202200511, https://doi.org/10.1002/anie.202200511.

[9] S. Riegsinger, R. Popescu, D. Gerthsen, C. Feldmann, *Chem. Mater.* **2024**, *36*, 10496–10503, https://doi.org/10.1021/acs.chemmater.4c01533.

[10] M. E. Arroyo-de Dompablo, A. Ponrouch, P. Johansson, M. R. Palacín, *Chem. Rev.* **2020**, *120*, 6331–6357, https://doi.org/10.1021/acs.chemrev.9b00339.

[11] H. V. K. Diyabalanage, R. P. Shrestha, T. A. Semelsberger, B. L. Scott, M. E. Bowden, B. L. Davis, A. K. Burrell, *Angew. Chem. Int. Ed.* **2007**, *46*, 8995–8997, https://doi.org/10.1002/anie.200702240.

[12] S. Harder, *Chem. Rev.* **2010**, *110*, 3852–3876, https://doi.org/10.1021/cr9003659.

[13] M.-J. Evans, C. Jones, *Chem. Soc. Rev.* **2024**, *53*, 5054–5082, https://doi.org/10.1039/D4CS00097H.

[14] B. Rösch, T. X. Gentner, J. Eyselein, J. Langer, H. Elsen, S. Harder, *Nature* **2021**, *592*, 717–721.

[15] S. Krieck, H. Görls, L. Yu, M. Reiher, M. Westerhausen, *J. Am. Chem. Soc.* **2009**, *131*, 2977–2985, https://doi.org/10.1021/ja808524y.

[16] L. P. Cramer, B. E. Schubert, P. S. Petite, S. C. Langford, J. T. Dickinson, *J. Appl. Phys.* **2005**, *97*, 074307, https://doi.org/10.1063/1.1862758.

[17] R. Bennewitz, C. Günther, M. Reichling, E. Matthias, S. Vijayalakshmi, A. V. Barnes, N. H. Tolk, *Appl. Phys. Lett.* **1995**, *66*, 320–322, https://doi.org/10.1063/1.113531.

[18] U. Sanyal, R. Datta, B. R. Jagirdar, *RSC Adv.* **2012**, *2*, 259–263.

[19] S. Krieck, M. Westerhausen, *Chem. unserer Zeit* **2009**, *43*, 384–390, https://doi.org/10.1002/ciuz.200900500.

[20] T.-C. Wu, H. Xiong, R. D. Rieke, *J. Org. Chem.* **1990**, *55*, 5045–5051, https://doi.org/10.1021/jo00304a016.

[21] M. S. Sell, M. V. Hanson, R. D. Rieke, *Synth. Commun.* **1994**, *24*, 2379–2386, https://doi.org/10.1080/00397919408019062.

[22] *Org. Synth.* **1995**, *72*, 147, https://doi.org/10.15227/orgsyn.072.0147.

[23] R. D. Rieke, M. V. Hanson, *Tetrahedron* **1997**, *53*, 1925–1956, https://doi.org/10.1016/S0040-4020(96)01097-6.

[24] J.-S. Lee, R. Velarde-Ortiz, A. Guijarro, R. D. Rieke, *J. Org. Chem.* **2000**, *65*, 5428–5430, https://doi.org/10.1021/jo000413i.

[25] P. Schüler, *Calciumorganic compounds – from curiosity to ubiquity (CalCub)*, PhD thesis, Friedrich-Schiller-Universität Jena, Jena **2022**.

[26] A. Egeberg, T. Block, O. Janka, O. Wenzel, D. Gerthsen, R. Pöttgen, C. Feldmann, *Small* **2019**, *15*, 1902321.

[27] C. Schöttle, P. Bockstaller, D. Gerthsen, C. Feldmann, *Chem. Commun.* **2014**, *50*, 4547–4550.

[28] F. Gyger, P. Bockstaller, D. Gerthsen, C. Feldmann, *Angew. Chem. Int. Ed.* **2013**, *52*, 12443–12447, https://doi.org/10.1002/anie.201305289.

[29] C. Schöttle, P. Bockstaller, R. Popescu, D. Gerthsen, C. Feldmann, *Angew. Chem. Int. Ed.* **2015**, *54*, 9866–9870.

[30] D. Bartenbach, O. Wenzel, R. Popescu, L.-P. Faden, A. Reiß, M. Kaiser, A. Zimina, J.-D. Grunwaldt, D. Gerthsen, C. Feldmann, *Angew. Chem. Int. Ed.* **2021**, *60*, 17373–17377, https://doi.org/10.1002/anie.202104955.

[31] C. Ritschel, C. Donsbach, C. Feldmann, *Chem. - Eur. J.* **2024**, *30*, e202400418, https://doi.org/10.1002/chem.202400418.

[32] V. K. LaMer, R. H. Dinegar, *J. Am. Chem. Soc.* **1950**,*72*, 4847–4854, https://doi.org/10.1021/ja01167a001.

[33] J. C. Schottmiller, A. J. King, F. A. Kanda, *J. Phys. Chem.* **1958**, *62*, 1446–1449, https://doi.org/10.1021/j150569a024.

[34] C. Camp, J. Arnold, *Dalton Trans.* **2016**, *45*, 14462–14498, https://doi.org/10.1039/C6DT02013E.

[35] S. P. Green, C. Jones, A. Stasch, *Science* **2007**, *318*, 1754–1757, https://doi.org/10.1126/science.1150856.

[36] C. Cui, H. W. Roesky, H.-G. Schmidt, M. Noltemeyer, H. Hao, F. Cimpoesu, *Angew. Chem. Int. Ed.* **2000**, *39*, 4274–4276, https://doi.org/10.1002/1521-3773(20001201)39:23⟨4274::AID-ANIE4274⟩3.0.CO;2-K.

[37] J. Mai, B. Rösch, N. Patel, J. Langer, S. Harder, *Chem. Sci.* **2023**, *14*, 4724–4734, https://doi.org/10.1039/D3SC00909B.

[38] J. Mai, B. Rösch, J. Langer, S. Grams, M. Morasch, S. Harder, *Eur. J. Inorg. Chem.* **2023**, *26*, e202300421.

[39] J. Smid, *J. Am. Chem. Soc.* **1965**, *87*, 3, 655–656, https://doi.org/10.1021/ja01081a048.

[40] J. J. Brooks, W. Rhine, G. D. Stucky, *J. Am. Chem. Soc.* **1972**, *94*, 7346–7351, https://doi.org/10.1021/ja00776a014.

[41] C. Melero, A. Guijarro, M. Yus, *Dalton Trans.* **2009**, 1286, https://doi.org/10.1039/b821119c.

[42] M. N. Bochkarev, I. L. Fedushkin, A. A. Fagin, H. Schumann, J. Demtschuk, *Chem. Commun.* **1997**, 1783–1784, https://doi.org/10.1039/a703603e.

[43] I. L. Fedushkin, M. N. Bochkarev, H. Schumann, L. Esser, *J. Organomet. Chem.* **1995**, *489*, 145–151, https://doi.org/10.1016/0022-328X(94)05145-2.

[44] M. González-Maupoey, V. Tabernero, T. Cuenca, *Coord. Chem. Rev.* **2009**, *253*, 1854–1881, https://doi.org/10.1016/j.ccr.2009.02.013.

[45] C. Moreno, A. Arnanz, S. Delgado, *Inorg. Chim. Acta* **2001**, *312*, 139–150, https://doi.org/10.1016/S0020-1693(00)00357-1.

[46] J. C. Smart, C. J. Curtis, *J. Am. Chem. Soc.* **1977**, *99*, 3518, https://doi.org/10.1021/ja00452a063.

[47] M. L. H. Green, V. S. B. Mtetwa, A. Sella, A. N. Chernega, *Dalton Trans.* **1994**, *2*, 201–207, https://doi.org/10.1039/DT9940000201.

[48] M. Carrondo, P. M. Matias, G. A. Jeffrey, *Acta Crystallogr. C* **1984**, *40*, 932–934, https://doi.org/10.1107/S0108270184006314.

[49] A. Coda, K. Prout, V. Tazzoli, *Acta Crystallogr. B* **1979**, *35*, 1597–1600, https://doi.org/10.1107/S0567740879007214.

[50] K. Prout, T. S. Cameron, R. A. Forder, S. R. Critchley, B. Denton, G. V. Rees, *Acta Crystallogr. B* **1974**, *30*, 2290–2304, https://doi.org/10.1107/S0567740874007011.

[51] P. Pyykkö, M. Atsumi, *Chem. - Eur. J.* **2009**, *15*, 186–197.
[52] B. Cordero, V. Gómez, A. E. Platero-Prats, M. Revés, J. Echeverría, E. Cremades, F. Barragán, S. Alvarez, *Dalton Trans.* **2008**, 2832, https://doi.org/10.1039/b801115j.
[53] K. Prout, R. A. Forder, *Acta Crystallogr. B* **1975**, *31*, 852–856, https://doi.org/10.1107/S0567740875003925.
[54] M. P. Blake, N. Kaltsoyannis, P. Mountford, *J. Am. Chem. Soc.* **2015**, *137*, 12352–12368, https://doi.org/10.1021/jacs.5b07866.
[55] S. Liu, B. A. Smith, J. K. Kirkland, K. D. Vogiatzis, G. S. Girolami, *Inorg. Chem.* **2021**, *60*, 8790–8801, https://doi.org/10.1021/acs.inorgchem.1c00737.
[56] J. A. Kelly, J. Gramüller, R. M. Gschwind, R. Wolf, *Dalton Trans.* **2021**, *50*, 13985–13992, https://doi.org/10.1039/D1DT02621F.
[57] S. Bajo, M. G. Alférez, M. M. Alcaide, J. López-Serrano, J. Campos, *Chem. - Eur. J.* **2020**, *26*, 16833–16845, https://doi.org/10.1002/chem.202003167.
[58] X. Jin, Y. Bai, Y. Zhou, G. Wang, L. Zhao, M. Zhou, G. Frenking, *Angew. Chem. Int. Ed.* **2021**, *60*, 13865–13870, https://doi.org/10.1002/anie.202103267.
[59] M. Zhou, G. Frenking, *Acc. Chem. Res.* **2021**, *54*, 3071–3082, https://doi.org/10.1021/acs.accounts.1c00277.
[60] P. Stegner, C. Färber, J. Oetzel, U. Siemeling, M. Wiesinger, J. Langer, S. Pan, N. Holzmann, G. Frenking, U. Albold, B. Sarkar, S. Harder, *Angew. Chem. Int. Ed.* **2020**, *59*, 14615–14620, https://doi.org/10.1002/anie.202005774.
[61] J. Pipek, P. G. Mezey, *J. Chem. Phys.* **1989**, *90*, 4916–4926, https://doi.org/10.1063/1.456588.
[62] O. Ekkert, A. J. P. White, M. R. Crimmin, *Angew. Chem. Int. Ed.* **2016**, *55*, 16031–16034, https://doi.org/10.1002/anie.201608599.
[63] H. Shen, E. Selenius, P. Ruan, X. Li, P. Yuan, O. Lopez-Estrada, S. Malola, S. Lin, B. K. Teo, H. Häkkinen, N. Zheng, *Chem. Europ. J.* **2020**, *26*, 8465–8470, https://doi.org/10.1002/chem.202001753.
[64] B. S. Gutrath, U. Englert, Y. Wang, U. Simon, *Europ. J. Inorg. Chem.* **2013**, *12*, 2002–2006.
[65] F. Fetzer, C. Schrenk, N. Pollard, A. Adeagbo, A. Z. Clayborne, A. Schnepf, *Chem. Commun.* **2021**, *57*, 3551–3554, https://doi.org/10.1039/D0CC07006H.
[66] A. Terahara, H. Ohya-Nishiguchi, N. Hirota, A. Oku, *J. Phys. Chem.* **1986**, *90*, 1564–1571, https://doi.org/10.1021/j100399a022.
[67] G. S. Owen, G. Vincow, *J. Chem. Phys.* **1971**, *54*, 368–375, https://doi.org/10.1063/1.1674618.
[68] Y. Li, R. Jin, *J. Am. Chem. Soc.* **2020**, *142*, 32, 13627–13644, https://doi.org/10.1021/jacs.0c05866.
[69] M. Agrachev, M. Ruzzi, A. Venzo, F. Maran, *Acc. Chem. Res.* **2019**, *52*, 44–52, https://doi.org/10.1021/acs.accounts.8b00495.
[70] C. L. Dodson, J. F. Graham, *J. Phys. Chem.* **1973**, *77*, 2903–2906, https://doi.org/10.1021/j100642a015.
[71] H. Torii, Y. Ueno, A. Sakamoto, M. Tasumi, *Can. J. Chem.* **2004**, *82*, 951–963, https://doi.org/10.1139/v04-050.
[72] A. E. Reed, R. B. Weinstock, F. Weinhold, *J. Chem. Phys.* **1985**, *83*, 735–746, https://doi.org/10.1063/1.449486.
[73] D. Michael, P. Mingos, *Pure Appl. Chem.* **1980**, *52*, 705–712.
[74] F. Fetzer, N. Pollard, N. C. Michenfelder, M. Strienz, A. N. Unterreiner, A. Z. Clayborne, A. Schnepf, *Angew. Chem. Int. Ed.* **2022**, *61*, e202206019, https://doi.org/10.1002/anie.202206019.
[75] J. Chen, Q.-F. Zhang, T. A. Bonaccorso, P. G. Williard, L.-S. Wang, *J. Am. Chem. Soc.* **2014**, *136*, 92–95, https://doi.org/10.1021/ja411061e.

Manuscript received: July 22, 2025
Revised manuscript received: October 08, 2025
Manuscript accepted: October 09, 2025
Version of record online: ■■, ■■